

A temperature-modulated dilatometer by using a piezobender-based device

Yanhong Gu,^{1,2} Bo Liu,^{1,2} Wenshan Hong,^{1,2} Zhaoyu Liu,^{1,3} Wenliang Zhang,^{1,4} Xiaoyan Ma,^{1,2, a)} and Shiliang Li^{1, 2, 5, b)}

¹⁾Beijing National Laboratory for Condensed Matter Physics, Institute of Physics, Chinese Academy of Sciences, Beijing 100190, China

²⁾School of Physical Sciences, University of Chinese Academy of Sciences, Beijing 100190, China

³⁾Department of Physics, University of Washington, Seattle, WA 98195, USA

⁴⁾Swiss Light Source, Paul Scherrer Institut, CH-5232 Villigen PSI, Switzerland

⁵⁾Songshan Lake Materials Laboratory, Dongguan, Guangdong 523808, China

(Dated: 24 May 2022)

We report a new design of temperature-modulated dilatometer, which obtains the linear thermal expansion coefficient by measuring the oscillating changes of the sample's length and temperature by a piezobender and a thermocouple, respectively. Using an iron-based superconductor KFe_2As_2 as an example, we show that this device is able to measure thin samples with high resolutions at low temperatures and high magnetic fields. Despite its incapability of giving absolute values, the new dilatometer provides a high-resolution method to study many important physical properties in condensed matter physics, such as thermal and quantum phase transitions, and vortex dynamics in the superconducting state. The prototype design of this device can be further improved in many aspects to meet particular requirements.

I. INTRODUCTION

The thermal expansion of a material describes the variation of its length or volume with temperature and is an fundamental thermodynamical parameter in studying the physical properties of solids¹. Especially, studying the change of thermal expansion across a phase transition has become one of the important techniques in condensed matter physics since it can reflect the intrinsic change of the electronic system with very high resolution²⁻⁶. In the case of studying superconductors, the thermal-expansion measurement can detect phase transitions and vortex dynamics within the superconducting state⁷⁻¹⁰, which shows its unique advantages compared to resistivity and magnetic-susceptibility measurements. The ratio between the thermal expansion and the specific heat gives the Grüneisen parameter, which is a crucial thermodynamical parameter for studying quantum critical transitions¹¹⁻¹⁶.

For low-temperature measurements in the field of condensed matter physics, the mostly used and accurate dilatometers are based on directly measuring the length change of a sample with temperature by a plate capacitor or based upon an atomic microscope piezocantilever¹⁷⁻²⁴. The linear thermal-expansion coefficient α can be directly derived from dL/LdT , where L and T are the length and temperature of the sample, respectively. Using alternating-current (AC) heating method, the thermal expansion can also be measured by temperature-modulated dilatometers (TMD), but previous reports only show measurements above room temperature²⁵⁻²⁷. The advantage of the TMD is that the setup is simple. The difficulty is how to measure the alternating length change of a sample at low temperatures.

In this work, we present a new design of TMD based on a piezobender device that can be used at low temperatures and high magnetic fields. It is based on the uniaxial pressure device as reported previously^{28,29}. With slightly changing the setup, we find that the device can be easily adapted to measure the linear thermal expansion. This method is similar to the temperature-modulated calorimetry (TMC) and other temperature-modulated measurements³⁰⁻³². The basic principle is to periodically heat a sample so that the oscillating changes of a sample's length and temperature, i.e., ΔL and ΔT , can be simultaneously determined with the assistance of a lock-in system. High resolutions can be thus achieved because of the capability of detecting small signals by the lock-in system. The linear thermal expansion α can be directly obtained as $\Delta L/L\Delta T$. We will use the iron-based superconductor KFe_2As_2 as an example to show the ability of our device of measuring the thermal expansion at low temperatures and high magnetic fields.

II. EXPERIMENTAL SETUP AND MEASUREMENT PRINCIPLES

Figure 1(a) and 1(b) show the sketch and the photo of the AC dilatometer, respectively, which is similar to the uniaxial pressure device reported previously²⁸. It is composed of a piezobender and a sapphire block secured by a CuBe frame. The two ends of a thin-slab sample are glued on top of them by GE varnish. The length of the sample is limited by the adjustable distance between the piezobender and the sapphire, which can be down to 0.5 mm for our device. The model of the piezobender is NAC2222 (Noliac) with the length, width and thickness as 21, 7.8 and 1.3 mm, respectively. There are three contacts for the piezobender and two side ones are soldered together. In using it as a uniaxial pressure device, a DC voltage is applied to the piezobender, which will tend to

^{a)}Electronic mail: mxy@iphy.ac.cn

^{b)}Author to whom correspondence should be addressed:slli@iphy.ac.cn

move it due to the reverse piezoelectric effect and thus provide a force on the sample. To measure the thermal expansion, a heater and a thermometer are attached to two sides of the sample by N grease, as shown in Fig. 1(a). The heater can be an external heater such as a resistor heater or the sample can be heated by itself with current flowing. The thermocouple made of Ni90/Cr10 and Au99.93/Fe0.07 wires was used as the thermometer. The setup in Fig. 1(a) was put on to the regular sample puck of the Physical Properties Measurement System (PPMS, Quantum Design) as shown in Fig. 1(b), which provides the low-temperature and magnetic-field environment. A lock-in system was used to provide the AC power and measure the signals from the thermometer and piezobender. The measurement diagram is shown in Fig. 1(c). In this work, we have used a two-channel lock-in system (Model OE1022D from SYSU Scientific Instruments) and two preamplifiers (Model SR560 from Stanford Research Systems).

Assuming that the AC current flowing through the heater with the resistance R has the form of $I_{AC} \sin \omega t$ and neglecting the phase change, the AC power supplied by it will be $P_{AC} \sin^2 \omega t$, where $P_{AC} = I_{AC}^2 R / 2$. This will result in an oscillating temperature of the sample, ΔT with the 2ω periodicity. With proper conditions, it has already been shown that the magnitude of ΔT , i.e. ΔT_{AC} , has the following form³⁰,

$$\Delta T_{AC} = \frac{P_{AC}}{2\omega C_s} \left[1 + \frac{1}{4\omega^2 \tau_1^2} + 4\omega^2 \tau_2^2 + \frac{2K_b}{3K_s} \right]^{-\frac{1}{2}}, \quad (1)$$

where C_s is the heat capacity of the sample, K_b is the thermal conductance between the sample and the bath, K_s is the thermal conductance of the sample, τ_1 is the relaxation time from sample to bath, τ_2 is associated with the time which the sample, the heater and the thermometer attain thermal equilibrium. The frequency-independent term $2K_b/3K_s$ is the geometric correction due to the finite thermal diffusivity of the sample. In the case where τ_1 is large while τ_2 and $2K_b/3K_s$ are small, ΔT_{AC} can take the much simpler form as

$$\Delta T_{AC} = \frac{P_{AC}}{2\omega C_s}, \quad (2)$$

which is the case for most traditional AC calorimeters.

The oscillating temperature of the sample will simultaneously cause the oscillation of its volume. The change of the length along a particular direction can be measured by the piezobender for the setup in Fig. 1(a) since the movement of the top will create a voltage that can be detected by the lock-in system. Figure 1(d) shows an example, where V_{sin} is the sine output voltage of the lock-in amplifier while V_{PB} is the voltage of the piezobender. It is clear that the periodicity of V_{PB} is twice of that of V_{sin} . Neglecting all the phase differences, the linear expansion coefficient α is thus

$$\alpha = \frac{\Delta L_{AC}}{L_0 \Delta T_{AC}} = \frac{\eta \kappa \Delta V_L}{L_0 \Delta T_{AC}}, \quad (3)$$

where L_0 is the static length of the sample between the tops of the BeCu frame and the piezobender, which is assumed to be a constant value since its change with temperature can

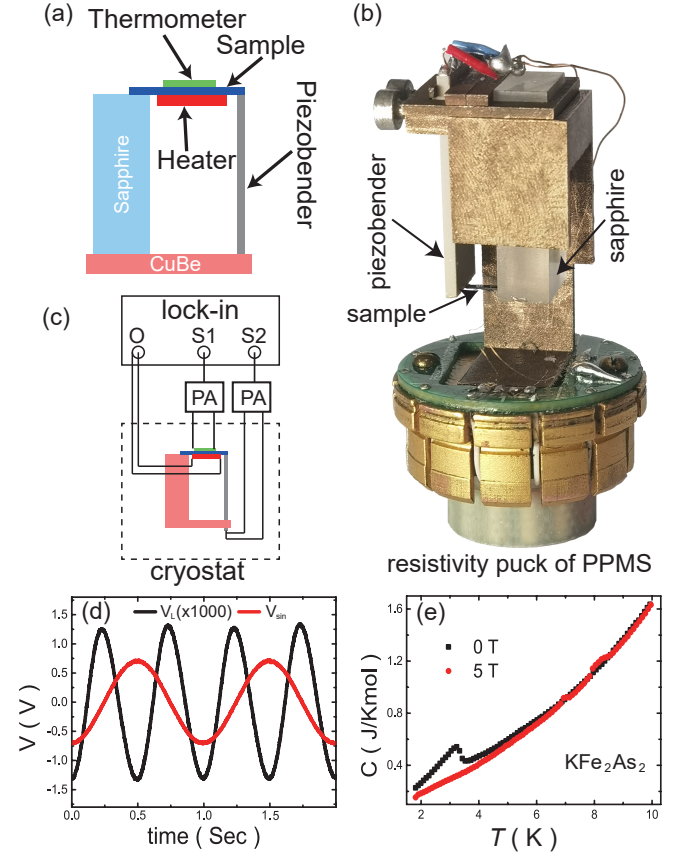


FIG. 1. (a) Sketch of the sample holder for AC dilatometer. The two ends of the sample are attached to the Sapphire block and piezobender, which are secured by a CuBe frame. A heater and a thermometer are attached to the two sides of the samples. (b) A photo of the AC dilatometer on the resistivity puck of the PPMS. The diameter of the puck is about 30 mm. The bottoms of the piezobender and the sapphire are separated by several plates, whose thickness can be changed to fit the sample's length. (c) Measurement diagram of the AC dilatometer. O, S1/S2 and PA represent the sineout and input channels of the lock-in amplifier, and the pre-amplifier, respectively. (d) The comparison of the waveforms of V_L (black line) and V_{sin} (red line). The frequency of the sine output voltage of the lock-in amplifier is 1 Hz. The temperature is 5 K. A preamplifier with 1000 gain has been used. (e) Temperature dependence of the specific heat for KFe_2As_2 at 0 (black squares) and 5 (red circles) Tesla.

be neglected. The magnitude of the oscillating length, ΔL_{AC} , is equal to $\eta \kappa \Delta V_L$, where ΔV_L is the magnitude of the oscillating voltage on the piezobender. The coefficient κ is the relationship between the moving distance of the top of the piezobender and the voltage resulted from, which has been independently determined to be about $(43.5 + 0.48T)$ nm/V below 10 K with the DC voltage supply³³. The coefficient η is introduced to account for other factors that may affect the determination of the length change. The value of η is hard to determine and we will give a rough estimation by comparing our results with those measured in the capacitive dilatometer.

The sample used here is an iron-based superconductor KFe_2As_2 . At $T_c = 3.4$ K, its thermal expansion along the a

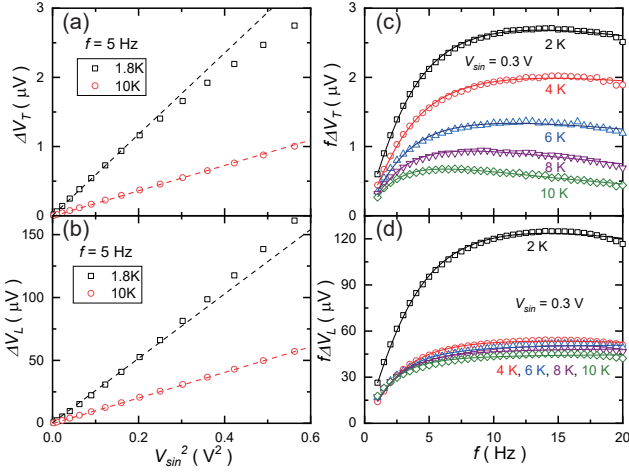


FIG. 2. (a) & (b) The V_{sin}^2 dependence of ΔV_T and ΔV_L , respectively. The frequency is fixed at 5 Hz. The temperatures are 10 and 1.8 K. The dashed lines are fitted by a linear function for $V_{sin} < 0.3$ V. (c) and (d) The frequency dependence of $f\Delta V_T$ and $f\Delta V_L$, respectively. The solid lines are the fitted results according to Eq. 1.

axis direction shows a drastic jump, changing from positive to negative value⁶. We grew the KFe_2As_2 samples by the flux method as reported previously³⁴. The specific heat shows a clear superconducting transition at 0 T, which disappears at 5 T, as shown in Fig. 1(e). Most of the thermal-expansion results were measured on a slice of the KFe_2As_2 sample, which was cut along the a axis with the length, width and thickness as 4, 0.85 and 0.14 mm, respectively. Two electronic contacts were made on the sample by silver epoxy. Because the resistance of the sample is very small ($< 10^{-3}\Omega$), it is the contact resistances that actually work as the heater. Some other KFe_2As_2 samples have also been measured to study the effect of sample size for some parameters.

III. RESULTS

According to Eq. (2) and (3), both the magnitudes of voltages from the thermocouple and the piezobender, ΔV_T and ΔV_L , should be proportional to the square of the magnitude of the heating voltage V_{sin} . As shown in Fig. 2(a) and 2(b), the quadratic relation holds for small voltages. At large voltages, ΔV_T becomes lower than the value from linear extrapolation. This is most likely due to the DC heating effect³¹, which results in an increase of the sample temperature and thus the increase of the specific heat and decrease of ΔT . To avoid this effect, V_{sin} is fixed as 0.3 V in the following measurements.

The frequency dependence of the ΔV_L and ΔV_T can be well described by Eq. 1 with the term $2K_b/3K_s$ neglected, as shown in Fig. 2(c) and 2(d), respectively. At low temperatures (2 and 4 K), $f\Delta V_T$ becomes frequency-independent at high frequencies, which is because τ_2 is very small (~ 2.1 ms). With increasing temperatures, τ_2 becomes larger so that its effect moves to lower frequencies and there is no frequency-independent region. For $f\Delta V_L$, the frequency-independent re-

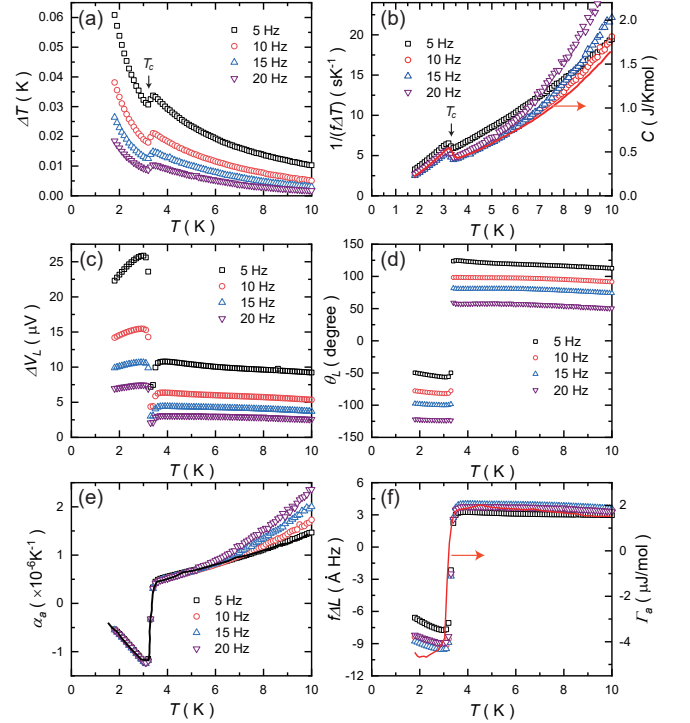


FIG. 3. (a) Temperature dependence of ΔT . (b) Temperature dependence of $1/(f\Delta T)$ and the specific heat (solid line). (c) & (d) Temperature dependence of ΔV_L and θ_L , respectively. (e) The temperature dependence of the linear temperature thermal expansion along the a axis α_a . The solid line is α_a from Ref.⁶. (f) The temperature dependence of the linear Gruneisen parameter. The solid line in (d) is Γ_a calculated by α from Ref.⁶ and the specific heat of KFe_2As_2 .

gion exists at all temperatures. The difference of τ_2 for ΔV_L and ΔV suggests that it takes longer time for the thermal couple to become thermal equilibrium since N-grease has been used to attach it to the sample. The frequency-independent region means that the signal has the form in Eq. 2, which suggests that the device works in the optimal condition for heat-capacity measurements in these frequencies.

Figure 3(a) shows the temperature dependence of ΔT , which is calculated by $\Delta V_T/S$ with S as the Seebeck coefficient of the thermocouple. It increases with decreasing temperature and shows a dip at T_c . According to Eq. 2, the specific heat should be proportional to $1/(f\Delta T)$ if the power P_{AC} has little temperature dependence. Figure 3(b) shows the comparison between $1/(f\Delta T)$ and the specific heat C . Below above 5 K, the data above 10 Hz closely follow the temperature dependence of C , which indicates the device is working at the optimal condition for the specific heat measurements. On the other hand, significant deviation occurs at higher temperatures, which is due to the increase of τ_2 for ΔV_T as discussed above.

Figure 3(c) shows the temperature dependence of ΔV_L , which shows a very sharp dip at T_c for all frequencies. This is because the linear thermal expansion coefficient α along the a axis changes sign at T_c ⁶. As shown in Fig. 3(d), the phase θ_L for ΔV_L changes exactly 180 degrees at T_c , which

demonstrates the sign change of ΔL across T_c . Except this 180-degree change, the value of θ_L has no physical meaning, so the change of length is only associated with ΔV_L .

Figure 3(e) shows the linear thermal expansion α_a along the a axis obtained by Eq. (3) with $\eta = 134$. The value of η is obtained by comparing our results with previous results measured by the capacitive dilatometer⁶. The origin of the large value of η will be discussed later. The temperature dependence of α_a below 5 K shows almost no frequency dependence and can be nicely normalized to the reported values. With increasing temperature, α_a becomes different for different frequencies, which is because the frequency dependence of ΔV_L and ΔV_T becomes different as shown in Figs. 2(c) and 2(d).

Figure 3(f) shows the temperature dependence $f\Delta L = f\eta\kappa\Delta V_L$ at different frequencies. The reason to plot this is that this value should be proportional to the linear Grüneisen parameter $\Gamma_a = \alpha_a/C_s$ according to Eq. 1 and 3. It is clear that the calculated values nicely follow the temperature dependence of Γ_a calculated from the α_a in Ref.⁶ and the specific heat. It should be noted that in this method, there is actually no need to measure ΔT . The absolute value of Γ_a can be obtained if the power P_{AC} can be determined.

IV. DISCUSSIONS

The above results demonstrate that it is possible to measure the thermal expansion at low temperatures by the AC method based on a piezobender device. There are several advantages compared to the capacitive dilatometer. First, the design and fabrication of the sample holder, and the experimental setup are very simple. The capacitive low-temperature dilatometer on the other hand is very specialized and its measurement needs high-resolution capacitance meter. Second, the device here can measure very thin crystals, which may be crucial for some materials where only thin slices of crystals are available. With the known spring constant of the piezobender (~ 0.0308 N/ μ m) and the Young's modulus (~ 105 GPa along the a axis for KFe_2As_2 ³⁵), we estimate that F/F' is about 100 for our sample used here, where F and F' are the force created by the thermal expansion of the sample and the force required to move the tip of the piezobender, respectively. This means that although the sample is thin, its thermal expansion is able to push the piezobender and create the voltage to be measured. In fact, the thinnest sample we have tried is about 18 μ m, which still has $F/F' \approx 30$. Third, the resolution is good as shown in Fig. 3(e) and (f). Based on the relative noise level of ΔV_L ($\sim 10^{-4}$) and the value of α_a , we estimate that the absolute resolution to resolve the length change of the sample is about 10^{-4} Å at 2 K. The resolution for α in this work is about 0.5×10^{-9} K⁻¹ at 2 K. It should be pointed out that better resolution can be achieved in the future by introducing better shielding and design of the electrical circuits, and different choices of the heater, the piezobender and the thermometer. Ideally, one may finally achieve a resolution better than $10^{-4}/\sqrt{f}$ Å at 2 K for the length change if the noise level of a lock-in system is about 2 nV/ \sqrt{f} .

As shown by this work, it is also possible to obtain the specific heat by our device as shown in Fig. 3(b). However, whether this is possible seems to depend on the sample thickness (and thus the mass), as for much thinner samples (~ 10 μ m), the measured C is about 10 times larger than the actual value, which may be because a large amount of heating power is applied on other part of the device. Nevertheless, the oscillating temperature of the sample can still be represented by ΔT and so the α value is still reliable. The simultaneous measurements of the linear thermal expansion α and the specific heat C_s of a sample means that one can obtain the linear Grüneisen parameter $\Gamma \propto \alpha/C_s$. In principle, even without the knowledge of ΔT and so the specific heat, it is still possible to directly obtain $\Gamma \propto \Delta V_L$ according to Eq. 2 and 3, as shown in Fig. 3(f), although it is still required that the measured C is close to C_s . We'd like to point it out though that in some cases where both C_s and Γ diverges, such as at a quantum critical point, ΔV_L still provides a good approximation to Γ .

There are several disadvantages for the TMD device here. First, it is hard to obtain the absolute value of α . As show above, the values measured here are more than two orders smaller than the actual ones. We have found that the relaxation time of the charges in the piezobender, which is about 20 ms at 2 K, makes the signal 4 times smaller than the maximum voltage created. Moreover, the output voltage of a piezobender strongly depends on frequency f and becomes much smaller when f is away from the resonance frequency³⁶⁻³⁸, which is about 1300 Hz for the piezobender used here. Fortunately, our results in Fig. 3(f) shows that for a fixed setup, η is independent of sample size, which means that the absolute value of α can be obtained by carefully comparing the results between the TMD and capacitive dilatometers. In fact, for the several KFe_2As_2 samples we have measured, the values of η are all around 140. Second, the device works well below 5 K where the optimal working condition described by Eq. 2 is satisfied. At higher temperatures, the effect of τ_2 in ΔT becomes significant, which results in the deviation of α_a from the linear temperature dependence (Fig. 3(e)). It is interesting to note that for ΔV_L , there is always a region that satisfy the optimal working condition as shown in Fig. 2(d). It follows that the τ_2 of the sample, i.e., the time which the sample attains thermal equilibrium, is much smaller than that of the thermocouple. If a thermometer with smaller heat capacity and better thermal conductance can be used, this issue may be solved.

Despite the above disadvantages, the TMD introduced here can be used to study some important physical properties, such as the phase transitions and vortex dynamics in the superconducting state. Especially, since the device works well below 5 K, it may be possible to apply it below 1.8 K to study quantum phase transitions. Moreover, although it is hard to obtain the absolute value, studying the systematic change of the thermal expansion in a particular system with doping and magnetic field etc is still reliable.

V. SUMMARY

We have designed a temperature-modulated dilatometer based on a piezobender device, which can measure the linear thermal expansion coefficient and in principle the Grüneisen parameter. Although it is hard to obtain the absolute values, the device has the capability of measuring very thin samples with high resolutions as illustrated by measuring KFe_2As_2 single crystals. Considering that this device is still a prototype, much improvements should be possible in the future.

ACKNOWLEDGMENTS

We thank great helps from Prof. Jing Guo. This work was supported by the National Key R&D Program of China (Grants No. 2017YFA0302903 and No. 2016YFA0300502), the National Natural Science Foundation of China (Grants No. 11874401 and No. 11674406), the Strategic Priority Research Program(B) of the Chinese Academy of Sciences (Grants No. XDB25000000 and No. XDB07020000, No. XDB28000000).

VI. DATA AVAILABILITY STATEMENT

The data that support the findings of this study are available from the corresponding authors upon reasonable request.

- ¹T. H. K. Barron, J. G. Collins, and G. K. White, “Thermal expansion of solids at low temperatures,” *Adv. Phys.* **29**, 609 (1980).
- ²G.-m. Zhao, M. B. Hunt, and H. Keller, “Strong oxygen-mass dependence of the thermal-expansion coefficient in the manganites $(\text{La}_{1-x}\text{Ca}_x)_{1-y}\text{Mn}_{1-y}\text{O}_3$,” *Phys. Rev. Lett.* **78**, 955–958 (1997).
- ³A. Bianchi, R. Movshovich, N. Oeschler, P. Gegenwart, F. Steglich, J. D. Thompson, P. G. Pagliuso, and J. L. Sarrao, “First-order superconducting phase transition in CeCoIn_5 ,” *Phys. Rev. Lett.* **89**, 137002 (2002).
- ⁴G. Motoyama, T. Nishioka, and N. K. Sato, “Phase transition between hidden and antiferromagnetic order in URu_2Si_2 ,” *Phys. Rev. Lett.* **90**, 166402 (2003).
- ⁵J. Hemberger, H.-A. K. von Nidda, V. Tsurkan, and A. Loidl, “Large magnetostriction and negative thermal expansion in the frustrated antiferromagnet ZnCr_2Se_4 ,” *Phys. Rev. Lett.* **98**, 147203 (2007).
- ⁶F. Hardy, A. E. Böhmer, D. Aoki, P. Burger, T. Wolf, P. Schweiss, R. Heid, P. Adelman, Y. X. Yao, G. Kotliar, J. Schmalian, and C. Meingast, “Evidence of strong correlations and coherence-incoherence crossover in the iron pnictide superconductor KFe_2As_2 ,” *Phys. Rev. Lett.* **111**, 027002 (2013).
- ⁷R. Modler, P. Gegenwart, M. Lang, M. Deppe, M. Weiden, T. Lühmann, C. Geibel, F. Steglich, C. Paulsen, J. L. Tholence, N. Sato, T. Komatsubara, Y. Ōnuki, M. Tachiki, and S. Takahashi, “First-order transition between weak and strong pinning in clean superconductors with enhanced spin susceptibility,” *Phys. Rev. Lett.* **76**, 1292–1295 (1996).
- ⁸R. Lortz, C. Meingast, U. Welp, W. K. Kwok, and G. W. Crabtree, “Crystal-lattice coupling to the vortex-melting transition in $\text{YBa}_2\text{Cu}_3\text{O}_{7-\delta}$,” *Phys. Rev. Lett.* **90**, 237002 (2003).
- ⁹S. Zaum, K. Grube, R. Schäfer, E. D. Bauer, J. D. Thompson, and H. v. Löhneysen, “Towards the identification of a quantum critical line in the (p, B) phase diagram of CeCoIn_5 with thermal-expansion measurements,” *Phys. Rev. Lett.* **106**, 087003 (2011).
- ¹⁰H. K. Mak, P. Burger, L. Cevey, T. Wolf, C. Meingast, and R. Lortz, “Thermodynamic observation of a vortex melting transition in the Fe-based superconductor $\text{Ba}_{0.5}\text{K}_{0.5}\text{Fe}_2\text{As}_2$,” *Phys. Rev. B* **87**, 214523 (2013).
- ¹¹L. Zhu, M. Garst, A. Rosch, and Q. Si, “Universally diverging Grüneisen parameter and the magnetocaloric effect close to quantum critical points,” *Phys. Rev. Lett.* **91**, 066404 (2003).
- ¹²T. Lorenz, O. Heyer, M. Garst, F. Anfuso, A. Rosch, C. Rüegg, and K. Krämer, “Diverging thermal expansion of the spin-ladder system $(\text{C}_5\text{H}_{12}\text{N})_2\text{CuBr}_4$,” *Phys. Rev. Lett.* **100**, 067208 (2008).
- ¹³J. G. Donath, F. Steglich, E. D. Bauer, J. L. Sarrao, and P. Gegenwart, “Dimensional crossover of quantum critical behavior in CeCoIn_5 ,” *Phys. Rev. Lett.* **100**, 136401 (2008).
- ¹⁴C. Meingast, F. Hardy, R. Heid, P. Adelman, A. Böhmer, P. Burger, D. Ernst, R. Fromknecht, P. Schweiss, and T. Wolf, “Thermal expansion and Grüneisen parameters of $\text{Ba}(\text{Fe}_{1-x}\text{Co}_x)_2\text{As}_2$: A thermodynamic quest for quantum criticality,” *Phys. Rev. Lett.* **108**, 177004 (2012).
- ¹⁵Y. Tokiwa, E. D. Bauer, and P. Gegenwart, “Zero-field quantum critical point in CeCoIn_5 ,” *Phys. Rev. Lett.* **111**, 107003 (2013).
- ¹⁶A. Steppke, R. KÜchler, S. Lausberg, E. Lengyel, L. Steinke, R. Borth, T. Lühmann, C. Krellner, M. Nicklas, C. Geibel, F. Steglich, and M. Brando, “Ferromagnetic quantum critical point in the heavy-fermion metal $\text{YbNi}_4(\text{P}_{1-x}\text{As}_x)_2$,” *Science* **339**, 933–936 (2013).
- ¹⁷G. M. Schmiedeshoff, A. W. Lounsbury, D. J. Luna, S. J. Tracy, A. J. Schramm, S. W. Tozer, V. F. Correa, S. T. Hannahs, T. P. Murphy, E. C. Palm, A. H. Lacerda, S. L. Bud’ko, P. C. Canfield, J. L. Smith, J. C. Lashley, and J. C. Cooley, “Versatile and compact capacitive dilatometer,” *Rev. Sci. Instrum.* **77**, 123907 (2006).
- ¹⁸R. KÜchler, T. Bauer, M. Brando, and F. Steglich, “A compact and miniaturized high resolution capacitance dilatometer for measuring thermal expansion and magnetostriction,” *Rev. Sci. Instrum.* **83**, 095102 (2012).
- ¹⁹S. Abe, F. Sasaki, T. Oonishi, D. Inoue, J. Yoshida, D. Takahashi, H. Tsujii, H. Suzuki, and K. Matsumoto, “A compact capacitive dilatometer for thermal expansion and magnetostriction measurements at millikelvin temperatures,” *Cryogenics* **52**, 452 (2012).
- ²⁰R. S. Manna, B. Wolf, M. de Souza, and M. Lang, “High-resolution thermal expansion measurements under helium-gas pressure,” *Rev. Sci. Instrum.* **83**, 085111 (2012).
- ²¹D. Inoue, D. Kaido, Y. Yoshikawa, M. Minegishi, K. Matsumoto, and S. Abe, “Thermal expansion and magnetostriction measurements using a high sensitive capacitive dilatometer at millikelvin temperatures,” *Journal of Physics: Conference Series* **568**, 032001 (2014).
- ²²R. KÜchler, C. Stingl, and P. Gegenwart, “A uniaxial stress capacitive dilatometer for high-resolution thermal expansion and magnetostriction under multiextreme conditions,” *Rev. Sci. Instrum.* **87**, 073903 (2016).
- ²³R. KÜchler, A. Wörl, P. Gegenwart, M. Berben, B. Bryant, and S. Wiedmann, “The world’s smallest capacitive dilatometer for high-resolution thermal expansion and magnetostriction in high magnetic fields,” *Rev. Sci. Instrum.* **88**, 083903 (2017).
- ²⁴L. Wang, G. M. Schmiedeshoff, D. E. Graf, J.-H. Park, T. P. Murphy, S. W. Tozer, E. Palm, J. L. Sarrao, and J. C. Cooley, “Application of an atomic force microscope piezocantilever for dilatometry under extreme conditions,” *Meas. Sci. Technol.* **28**, 065006 (2017).
- ²⁵K. Uchino and L. E. Cross, “A very high sensitivity ac dilatometer for the direct measurement of piezoelectric and electrostrictive constants,” *Ferroelectrics* **27**, 35 (1980).
- ²⁶T. H. Johansen, “An AC dilatometer for linear expansivity measurement,” *High Temperature High Pressure* **19**, 77 (1987).
- ²⁷J. Su, P. Moses, and Q. M. Zhang, “A bimorph based dilatometer for field induced strain measurement in soft and thin free standing polymer films,” *Rev. Sci. Instrum.* **69**, 2480 (1998).
- ²⁸Z. Liu, Y. Gu, W. Zhang, D. Gong, W. Zhang, T. Xie, X. Lu, X. Ma, X. Zhang, R. Zhang, J. Zhu, C. Ren, L. Shan, X. Qiu, P. Dai, Y.-f. Yang, H. Luo, and S. Li, “Nematic quantum critical fluctuations in $\text{BaFe}_{2-x}\text{Ni}_x\text{As}_2$,” *Phys. Rev. Lett.* **117**, 157002 (2016).
- ²⁹Y. Gu, Z. Liu, T. Xie, W. Zhang, D. Gong, D. Hu, X. Ma, C. Li, L. Zhao, L. Lin, Z. Xu, G. Tan, G. Chen, Z. Y. Meng, Y.-f. Yang, H. Luo, and S. Li, “Unified phase diagram for iron-based superconductors,” *Phys. Rev. Lett.* **119**, 157001 (2017).
- ³⁰P. F. Sullivan and G. Seidel, “Steady-state, ac-temperature calorimetry,” *Phys. Rev.* **173**, 679–685 (1968).
- ³¹E. Gmelin, “Classical temperature-modulated calorimetry: A review,” *Thermochim. Acta* **304–305**, 1 (1997).

- ³²M. S. Ikeda, J. A. W. Straquadine, A. T. Hristov, T. Worasaran, J. C. Palmstrom, M. Sorensen, P. Walmsley, and I. R. Fisher, "AC elastocaloric effect as a probe for thermodynamic signatures of continuous phase transitions," *Rev. Sci. Instrum.* **90**, 083902 (2019).
- ³³X. Ma and S. Li, Unpublished.
- ³⁴Z. Liu, Y. Gu, W. Hong, T. Xie, D. Gong, X. Ma, J. Liu, C. Hu, L. Zhao, X. Zhou, R. M. Fernandes, Y.-f. Yang, H. Luo, and S. Li, "Nonlinear uniaxial pressure dependence of T_c in iron-based superconductors," *Phys. Rev. Research* **1**, 033154 (2019).
- ³⁵F. F. Tafti, J. P. Clancy, M. Lapointe-Major, C. Collignon, S. Faucher, J. A. Sears, A. Juneau-Fecteau, N. Doiron-Leyraud, A. F. Wang, X.-G. Luo, X. H. Chen, S. Desgreniers, Y.-J. Kim, and L. Taillefer, "Sudden reversal in the pressure dependence of T_c in the iron-based superconductor CsFe_2As_2 : A possible link between inelastic scattering and pairing symmetry," *Phys. Rev. B* **89**, 134502 (2014).
- ³⁶S. Roundy and P. K. Wright, "A piezoelectric vibration based generator for wireless electronics," *Smart Mater. Struct.* **13**, 1131 (2004).
- ³⁷J. Ajitsaria, S. Y. Choe, D. Shen, and D. J. Kim, "Modeling and analysis of a bimorph piezoelectric cantilever beam for voltage generation," *Smart Mater. Struct.* **16**, 447 (2007).
- ³⁸E. K. Reilly, F. Burghardt, R. Fain, and Paul Wright, "Powering a wireless sensor node with a vibration-driven piezoelectric energy harvester," *Smart Mater. Struct.* **20**, 125006 (2011).